J Amer Oil Chem Soc (2007) 84:219–227
DOI 10.1007/s11746-006-1034-0

ORIGINAL PAPER

Binary Phase Behavior of 1,3-Dipalmitoyl-2-oleoyl-*sn*-glycerol and 1,2-Dioleoyl-3-palmitoyl-*rac*-glycerol

L. Zhang · S. Ueno · S. Miura · K. Sato

Received: 9 August 2006 / Accepted: 15 December 2006 / Published online: 23 January 2007

Abstract 1,3-Dipalmitoyl-2-oleoyl-*sn*-glycerol (POP) and 1,2-dioleoyl-3-palmitoyl-*rac*-glycerol (OOP) are two major molecular species that account for roughly half of the total triacylglycerols in palm oil. The binary phase behavior of a POP/OOP mixture plays an important role in the crystallization of palm oil. We conducted thermodynamic and kinetic studies of OOP and its mixtures with POP using differential scanning calorimetry and X-ray diffraction with a conventional generator and synchrotron radiation. We found that OOP has two polymorphs, α as a metastable form and β' as the most stable form, and that the two forms are stacked in a triple-chain-length structure. The POP/OOP mixtures exhibited immiscible eutectic natures in both their metastable and their most stable states, in contrast to POP/1,2-dipalmitoyl-3-oleoyl-*rac*-glycerol and POP/1,3-dioleoyl-2-palmitoyl-*sn*-glycerol mixtures, in which molecular compounds of a double-chain-length structure were formed. A time-resolved synchrotron radiation X-ray diffraction study undertaken during the cooling and heating processes indicated that the α and β' forms of the POP and OOP fractions crystallized and melted in separate manners, and that crystallization of the β' form and the polymorphic transformation from α to β' of POP and OOP are promoted in the presence of another component. The absence of molecular compound crystals in the binary mixtures of POP/OOP is explained by taking into account the molecular interactions of acyl chain packing, glycerol conformation, and methyl end stacking, among which glycerol conformation appeared to be most influential.

Keywords Binary phase behavior · 1,3-Dipalmitoyl-2-oleoyl-*sn*-glycerol · 1,2-Dioleoyl-3-palmitoyl-*rac*-glycerol · Polymorphism · Differential scanning calorimetry · X-ray diffraction · Palm oil

Introduction

The natural fats present in biotissues and food materials are mixtures of different types of triacylglycerols (TAGs) [1]. The physical properties of fats are strongly determined by the polymorphic behavior and intersolubility of the major component TAGs, as evidenced in milk fats [2]. A physical analysis of real fat systems usually starts with understanding the properties of the individual component TAG molecules and subsequently progresses to their mixture systems; the latter of which typically begins with studying the binary systems of the major component TAGs. Various phase diagrams of binary mixtures of TAGs have been

L. Zhang
School of Food and Biological Engineering,
Zhengzhou University of Light Industry,
Zhengzhou, China

S. Ueno · K. Sato (✉)
Graduate School of Biosphere Sciences,
Hiroshima University,
Higashi-Hiroshima 739-8528, Japan
e-mail: kyosato@hiroshima-u.ac.jp

S. Miura
Technology and Research Institute,
Snow Brand Milk Products Co., Ltd.,
Kawagoe, Saitama, Japan

reviewed [3–5], but much still remains to be clarified. Few studies have been done on binary mixtures of symmetric and asymmetric mixed-acid TAGs in particular, which are abundantly present in natural fats and oils.

Three typical phases can occur in the phase behavior of binary mixtures: the solid solution phase, the eutectic phase, and molecular compound formation. The formation of a molecular compound has been observed in some binary systems of symmetric saturated–unsaturated mixed-acid TAGs, such as 1,3-distearoyl-2-oleoyl-*sn*-glycerol (SOS)/1,3-dioleoyl-2-stearoyl-*sn*-glycerol (OSO) [6] and 1,3-dipalmitoyl-3-oleoyl-*sn*-glycerol (POP)/1,3-dioleoyl-2-palmitoyl-*sn*-glycerol (OPO) [3, 7]. Molecular compound formations have also been observed in some binary mixtures between symmetric and asymmetric saturated–unsaturated mixed-acid TAGs, such as SOS/1,2-distearoyl-3-oleoyl-*rac*-glycerol (SSO) [8, 9] and POP/1,2-dipalmitoyl-3-oleoyl-*rac*-glycerol (PPO) [10]. The molecular compound in each mixture was formed at a 1:1 concentration ratio, indicating specific molecular interactions through the acyl chain moieties. Interestingly, the chain-length structure converted from triple (for the component TAGs of POP, OPO, PPO, SOS, OSO, and SSO) to double (a molecular compound). It is understood that specific interactions may differ between oleoyl chains and saturated acid chains, causing formation of a molecular compound with a double-chain-length structure. It would be interesting to examine a mixture of POP and 1,2-dioleoyl-3-palmitoyl-*rac*-glycerol (OOP), which together account for roughly half of the total TAGs in palm oil to confirm this.

Moran [3] described the formation of a molecular compound in a POP/OOP mixture, but the details were unclear. We examined the phase behavior of binary mixtures of POP and OOP in metastable and stable conditions in the present study using differential scanning calorimetry (DSC) and synchrotron radiation X-ray diffraction (XRD) methods. In contrast to the POP/OPO and POP/PPO mixtures, no molecular compound was revealed under any conditions. This indicates that formation of a molecular compound may occur not only through molecular interactions between the fatty acid chains but also through interactions of the glycerol groups.

Clarifying the phase behavior of mixtures of POP and OOP has practical importance for dry fractionation of palm oil [11]. Furthermore, a POP/OOP binary mixture may play an important role in the formation of granular crystals in margarine that contains palm oil based solid fats [12, 13].

Experimental Procedures

POP and OOP were purchased from Sigma Chemical Co. (St. Louis, MO, USA) at 99% purity and were used without further purification. Binary mixtures of POP and OOP were prepared by mixing the weighed samples at room temperature, melting them above 50 °C, mixing using a vortex mixer, rapidly cooling to 0 °C, and then tempering at different temperatures. Thermodynamic equilibration to obtain the most stable forms was performed by incubating the crystallized mixture samples at 12 °C for 3 months.

The transformation and melting behavior of the mixtures were measured by DSC (DSC-8240 and DSC-8230, Rigaku Co., Tokyo, Japan) at a rate of 2 and 5 °C/min. The crystal forms in the most stable states were measured by powder XRD (RINT-TTR, Rigaku Co., Tokyo, Japan, $\lambda = 0.154$ nm) using a rotator-anode X-ray beam generator. Synchrotron radiation XRD (SR-XRD, $\lambda = 0.150$ nm) was used to observe the kinetic processes of crystallization and melting in the metastable states using two beam lines, BL-9C and BL-15A, at the synchrotron radiation facility (Photon Factory, PF) at the National Laboratory for High-Energy Physics in Tsukuba, Japan. The PF operates at 2.5 GeV. The XRD spectra were recorded every 10 and 30 s with two gas-filled one-dimensional position-sensitive proportional counters Rigaku Co., Tokyo, Japan) that were placed for the small-angle region (512 channels over a total length of 200 mm) and for the wide-angle region (512 channels over a total length of 100 mm). The camera lengths, the distance between the samples and the detectors, were 1,100 mm (small angle) and 280 mm (wide angle). The temperatures of the samples were changed with a Mettler DSC-FP84 (Columbus, USA) for the slow cooling rate (5 °C/min) and with a Linkam LK-600PM (Cambridge, UK) for the rapid cooling rate (100 °C/min).

Results and Discussion

Phase Behavior in the Most Stable States

Figure 1a depicts DSC heating thermograms obtained at a rate of 2 °C/min for the most stable forms of the POP/OOP mixtures at various concentration ratios. The onset, offset, and peak top temperatures, which were used to construct the phase diagram shown in Fig. 1b, were defined as indicated in the inset in Fig. 1a. Single endothermic peaks were observed for pure OOP and POP, corresponding to melting of the β' form of OOP and the β form of POP. A single endothermic

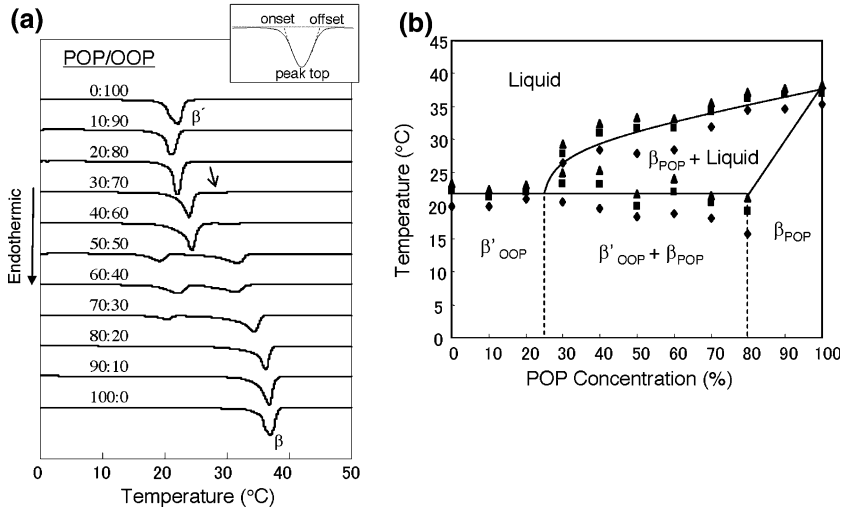

Fig. 1 **a** Differential scanning calorimetry (*DSC*) heating thermograms of 1,3-dipalmitoyl-3-oleoyl-*sn*-glycerol (*POP*)/1,2-dioleoyl-3-palmitoyl-*rac*-glycerol (*OOP*) mixtures in the most stable states. **b** Phase diagrams based on melting profiles with onset (*diamonds*), peak top (*squares*), and offset (*triangles*) temperatures

peak of OOP appeared in the mixtures of POP/OOP at 10:90 and 20:80 concentration ratios. The small, new endothermic peak indicated by an arrow was detectable in the mixture of POP/OOP at 30:70 concentration ratio, and increased in temperature with increasing concentration of POP. Therefore, this peak was due to the melting of the β form of POP. The melting peaks of the OOP fractions were not detectable in the mixtures containing OOP concentrations of 20 and 10%. We used the melting points in Fig. 1a to construct the phase diagram of the POP and OOP binary mixture in Fig. 1b, which reveals the eutectic nature. The minor components were solubilized into the major components at concentrations of POP and OOP lower than 20%.

Figure 2 presents XRD patterns of the most stable forms of POP/OOP binary mixtures obtained using the rotator-anode X-ray beam generator. The small-angle diffraction patterns of 3.04 nm (POP) and 3.27 nm (OOP) correspond to the (002) reflection of the long-spacing values of 6.08 and 6.54 nm of a triple-chain-length structure. Pure OOP exhibited distinct diffraction peaks in wide-angle X-ray scattering (WAXS) patterns of $2\theta = 22.5°$ and 20.5°, revealing the presence of lattice spacing of 0.40 and 0.43 nm. These patterns are characteristic of an orthorhombic perpendicular ($O_{\perp}$) subcell structure, and thus the most stable polymorphic form of OOP was the β' form. This result is consistent with that of the previous study [13]. Pure POP exhibited WAXS patterns of the β form, as reported in a previous study [14].

Mixing the two samples produced no new long-spacing peak in any of the ratios of POP/OOP examined. This contrasts with the XRD patterns obtained for mixtures of POP/OPO [7] and POP/PPO [10], in both of which new long-spacing patterns corresponding to the formation of the molecular compounds appeared and increased in intensity compared with those of the component TAGs when the concentration ratios of POP/OPO or POP/PPO approached 1:1. The short-spacing pattern exhibited a strong peak of 0.46 nm in the mixtures with POP concentrations over 50%, including 100% POP, which corresponds to a triclinic parallel ($T_{\parallel}$) subcell, indicating the occurrence of the β form of POP. The XRD patterns of the mixtures with POP concentrations of 80 and 90% were very similar to those of pure POP. The XRD patterns below a 50% POP concentration were very similar to those of the β' polymorph of OOP. The corresponding XRD patterns of POP are not detectable in Fig. 2, despite the presence of the DSC melting peaks of POP in the mixtures of POP/OOP at 30:70 and 40:60 concentration ratios. One reason for the difference is that DSC is a dynamic technique, so the β form of POP observed could have been formed during the DSC experiment. In contrast, the XRD pattern shown in Fig. 2 was taken at equilibrium.

We constructed the phase diagram in Fig. 1b to illustrate the coexistence of the β' form of OOP and the β form of POP, based on the DSC and XRD experiments.

Phase Behavior in Metastable States

Figure 3a illustrates the occurrence of metastable forms in the POP/OOP mixtures and presents DSC heating thermograms obtained at a heating rate of 5 °C/min soon after cooling the mixture samples from 40 to –30 °C at a rate of 5 °C/min. Figure 3b summarizes the kinetic phase behavior of the metastable forms using

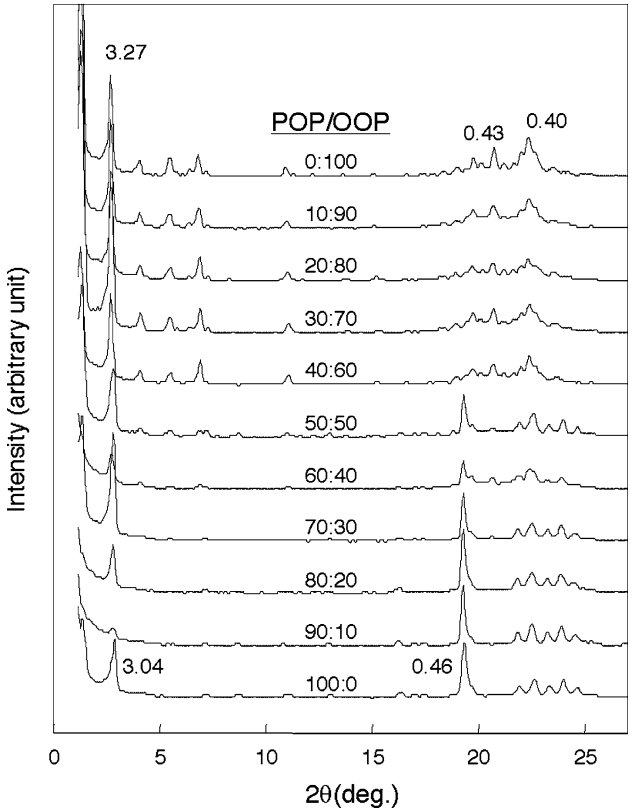

Fig. 2 X-ray diffraction (*XRD*) patterns of the most stable states of the POP/OOP mixtures crystallized at 12 °C for 3 months. The long-spacing and the short-spacing values are in nanometers

the DSC results provided in Fig. 3a and data from time-resolved SR-XRD experiments. Figure 4 presents the SR-XRD patterns of pure OOP and POP. The SR-XRD patterns of typical POP/OOP mixtures are depicted in Figs. 5, 6, and 7.

As indicated in Fig. 3a, the DSC heating thermogram of pure OOP exhibited a broad exothermic peak around –15 °C (indicated by arrow 1) and a sharp endothermic peak at 20 °C. Similar DSC patterns were observed in mixtures with OOP concentrations up to 20%. Figure 4a presents the SR-XRD patterns of OOP obtained during cooling and heating processes between 30 and –30 °C at a rate of 5 °C/min. Isothermal treatment was performed at –30 °C for 5 min before heating. An α form with a long-spacing value of 5.7 nm and a short-spacing value of 0.42 nm appeared during the cooling process. The α form then transformed to a β' form with a long-spacing value of 6.4 nm and short-spacing values of 0.45, 0.43, and 0.40 nm upon heating; further heating caused melting of the β' form around 22 °C. These results are basically consistent with those of the previous study [13]. The transformation from α to β' occurred over a wide range of temperatures between –15 and 10 °C, as revealed in the variation of the long- and short-spacing patterns in Fig. 4a. This result corresponded well with the broad exothermic peak of DSC indicated by arrow 1 in Fig. 3a.

As shown in Fig. 3a, the DSC heating thermogram of pure POP exhibited a sharp endothermic peak followed by a sharp exothermic peak around 14–16 °C, a large endothermic peak at 25 °C, and a small endothermic peak at 32 °C. The SR-XRD patterns (Fig. 4b) obtained during the cooling and heating processes between 40 and –30 °C at a rate of 5 °C/min revealed that an α form with long- and short-spacing values of 4.7 and 0.42 nm was produced by cooling and that melt-mediated $\alpha \rightarrow \gamma$ transformation occurred around 14 °C. This transformation was revealed in the SR-XRD patterns as the disappearance

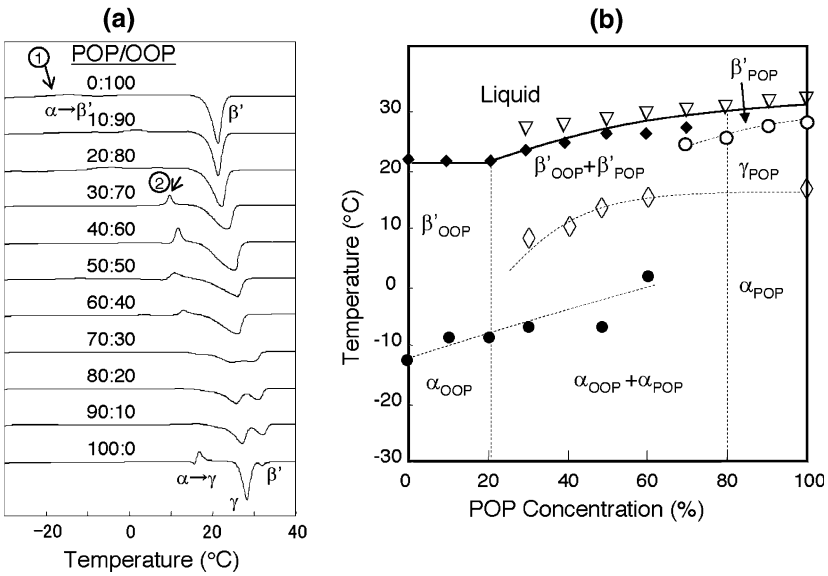

Fig. 3 **a** DSC heating thermograms (5 °C/min) and **b** kinetic phase behavior of POP/OOP mixtures. Melting points of α_{OOP} (*filled circles*), β'_{OOP} (*filled diamonds*), α_{POP} (*open diamonds*), β'_{POP} (*triangles*), and γ_{POP} (*open circles*)

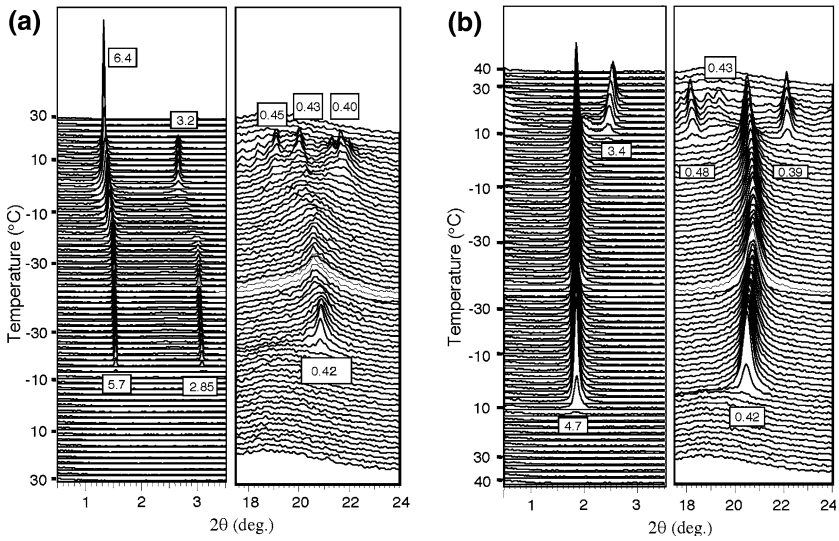

Fig. 4 Synchrotron radiation XRD patterns of crystallization, transformation, and melting of metastable forms of **a** OOP and **b** POP, obtained during cooling and heating processes at a rate of 5 °C/min

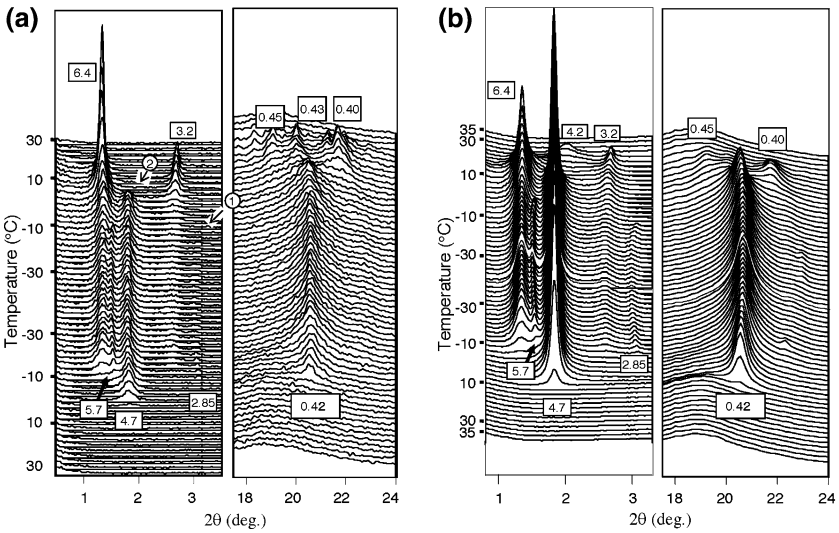

Fig. 5 Synchrotron radiation XRD patterns of crystallization, transformation, and melting of metastable forms of the mixtures of **a** POP/OOP at 30:70 concentration ratio and **b** POP/1,3-dioleoyl-2-palmitoyl-*sn*-glycerol (*OPO*) at 60:40 concentration ratio, obtained during cooling and heating processes at a rate of 5 °C/min

of the long- and short-spacing patterns of the α form at 14 °C, which was soon followed by a long-spacing pattern of 3.4 nm (002 reflection) and short-spacing values of 0.48 and 0.39 nm. These XRD patterns are characteristic of the γ form of POP in a triple-chain-length structure [14]. Further heating caused the XRD patterns of the γ form to disappear around 27 °C and the gradual appearance of the β' form with a short-spacing pattern of 0.43 nm in the double-chain-length structure [14], which then disappeared at around 30 °C owing to melting. Although there were subtle discrepancies in the melting temperatures, there was good agreement between the results obtained by DSC and SR-XRD for the basic features of crystallization and transformation of POP.

We confirmed that the SR-XRD patterns of the mixtures of POP/OOP at 10:90 and 20:80 concentration ratios and those of mixtures of POP/OOP at 80:20 and 90:10 concentration ratios were basically the same as those of pure OOP and POP (result not shown). This indicates that the fractions of POP and OOP in the former and latter mixtures are solubilized in the crystals of OOP and POP.

Concurrent crystallization of the OOP and POP fractions was clearly observed in the mixtures of POP/OOP at 30:70, 40:60, 50:50, and 60:40 concentration ratios. Peculiar properties commonly observed in the DSC results of the four mixtures included exothermic peaks around 10–13 °C and broad endothermic peaks around 15–28 °C. For example, the heating thermo-

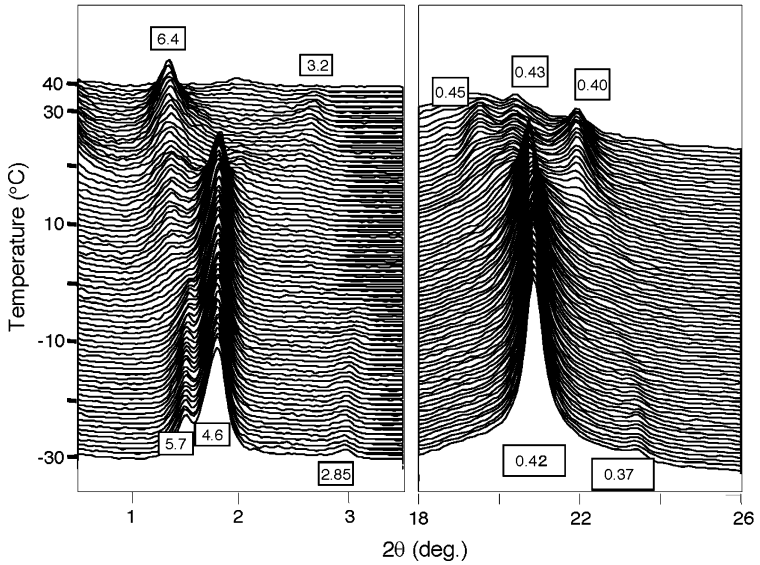

Fig. 6 Synchrotron radiation XRD patterns of a POP/OOP mixture at 60:40 concentration ratio obtained during heating at a rate of 5 °C/min after quenching from 40 to –30 °C at a rate of 100 °C/min

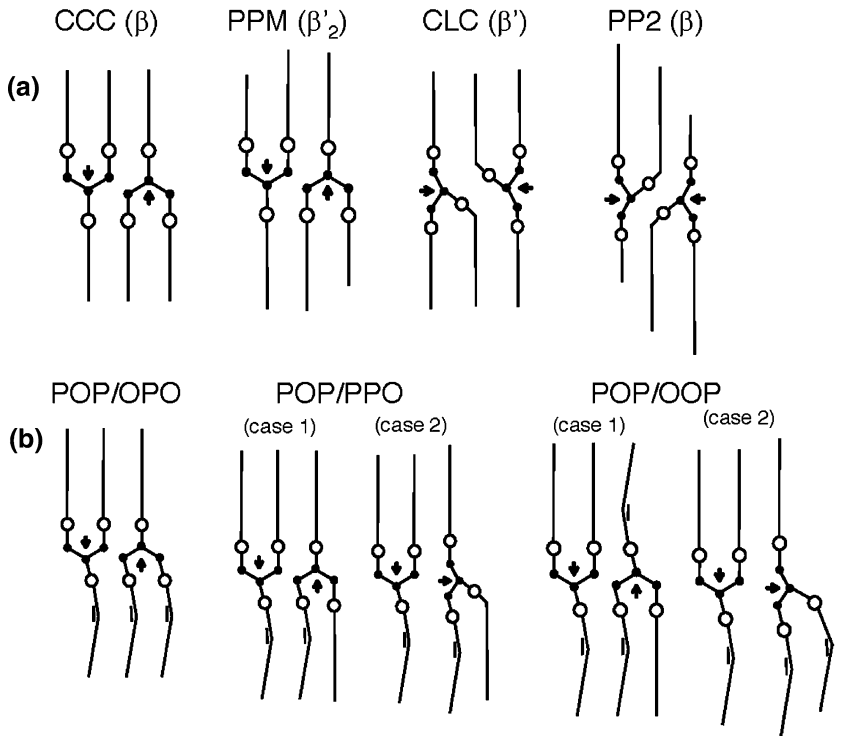

Fig. 7 Structure models close to the glycerol groups of **a** principal triacylglycerols whose atomic-level crystal structures were analyzed and **b** possible structures of molecular compound crystals. *CCC* tricaproylglycerol, *PPM* 1,2-dipalmitoyl-3-myristoyl-*sn*-glycerol, *CLC* 1,3-dicaproyl-*sn*-2-lauroylglycerol, *PP2* 1,2-dipalmitoyl-3-acetyl-*sn*-glycerol

grams for the mixture of POP/OOP at 30:70 concentration ratio revealed a small exothermic peak at 10 °C, as indicated by arrow 2 in Fig. 3a. The same peaks were observed in the mixtures of POP/OOP at 40:60, 50:50, and 60:40 concentration ratios. The SR-XRD experiments proved that these peaks correspond to the solid-state transformation from α to β' of the POP fraction that was crystallized separately from the OOP fractions, and that the broad endothermic peaks around 15–28 °C were due to superposition of the melting of the β' form of the POP and OOP fractions. Furthermore, the SR-XRD experiments clarified that the crystallization and polymorphic transformation of the OOP fractions differed significantly from those observed in pure OOP and the mixtures with POP concentrations of 10 and 20%.

Figure 5a presents the SR-XRD patterns of the mixture of POP/OOP at 30:70 concentration ratio obtained by cooling and heating between 30 and –30 °C when isothermal treatment was performed for

5 min before heating. The small-angle X-ray scattering (SAXS) patterns clearly indicated separate crystallization and transformation of the POP and OOP fractions, whereas the WAXS patterns representing the subcell structures of the α and β' forms did not differ between POP and OOP. The α form of POP with a long spacing of 4.7 nm and a short spacing of 0.42 nm crystallized first, around 5 °C during the cooling process. Subsequently, the α form of OOP with long spacings of 5.7 nm (001 reflection) and 2.85 nm (002 reflection) crystallized at –10 °C. Further cooling caused crystallization of the β' form of OOP with long spacings of 6.4 nm (001 reflection) and 3.2 nm (002 reflection) at –14 °C. This pattern continued to occur throughout the cooling and heating processes. The α form of OOP transformed to the β' form at –10 °C during the heating process, as revealed by the disappearance of the XRD patterns of 5.7 and 2.85 nm (see arrow 1 in Fig. 5a). The α form of the POP fraction transformed to the β' form around 8 °C, as indicated by arrow 2. The SAXS peak of 4.7 nm and the WAXS peak of 0.42 nm disappeared at this temperature and the SAXS peaks of 6.4 and 3.2 nm increased in intensity, indicating that the β' form of POP thus transformed from the α form was a triple-chain-length structure. At the same time, the WAXS patterns of 0.45, 0.43, and 0.40 nm appeared at the expense of the peak of 0.42 nm. Therefore, the β' forms of the OOP and POP fractions were present above 8 °C, with both melting around 24–27 °C.

Figure 5b presents SR-XRD patterns of the mixture of POP/OOP at 60:40 concentration ratio obtained by cooling and heating between 35 and –30 °C when isothermal treatment was performed for 5 min before heating. The α form of POP and the α and β' forms of OOP appeared during the cooling process. The α form of OOP transformed to the β' form during the heating process at around 0 °C, and melt-mediated $\alpha \rightarrow \beta'$ transformation of POP occurred around 14 °C. The β' forms of OOP and POP melted around 20–27 °C. These features are very similar to those of the POP/OOP mixture at 30:70 concentration ratio in Fig. 5a. However, the long spacing of 4.2 nm of the POP fraction appeared around 30 °C and this form was a double-chain-length structure. The same result (not shown here) was observed for the POP fractions in mixtures containing 10–30% POP.

The following properties were notable in a comparison of the transformation properties of OOP and POP fractions in mixtures of POP/OOP at 30:70 and 60:40 concentration ratio with those in the pure materials.

1. OOP crystallized in the α form in the pure state without occurrence of the β' form; it then transformed to the β' form during the heating process. However, concurrent occurrence of α and β' forms of OOP was observed in the mixture states, not only in the mixtures of POP/OOP at 30:70 and 60:40 concentration ratio, shown in Fig. 5, but also in the mixtures of POP/OOP at 40:60, 50:50, and 70:30 concentration ratios (not shown).
2. POP revealed a transformation from α to γ in the pure state through melt mediation, and the γ form transformed to the β' form during further heating. However, the γ form did not occur in the mixture states.
3. The β' form of POP in the mixture was a triple-chain-length structure when the concentration of POP was low, whereas a β' form with a double-chain-length structure was formed with increasing concentration of POP in the mixture. This result indicates the influence of POP on the stabilization of the β' form with the double-chain-length structure of the palm oil midfraction that contains about 70–80% of POP.

The second and third properties may be due to molecular interactions between POP and OOP, since OOP does not have a γ form and its β' form is a triple-chain-length structure. The first property may be due to the kinetic effect of the crystallization rate. An SR-XRD experiment was carried out to confirm this by rapidly cooling the mixture sample before heating.

Figure 6 presents SR-XRD patterns of the POP/OOP mixture at 60:40 concentration ratio obtained during heating after quenching the mixture sample from 40 to –30 °C at a rate of 100 °C/min using the Linkam LK–600PM. Only the α form was produced in both OOP and POP at –30 °C, and it transformed to the β' form at –4 °C in OOP and at 20 °C in POP. The occurrence of a short spacing of 0.37 nm may have been due to the occurrence of a sub-α form during the very high rate of cooling. This result indicates that the occurrence and transformation of metastable forms are sensitive to the rate of cooling owing to kinetic effects.

The kinetic phase behavior is summarized in Fig. 3b based on the DSC thermograms in Fig. 3a and the SR-XRD experiments performed at a cooling and heating rate of 5 °C/min. Eutectic phase behavior was observed in both the α form and the β' form and was similar to that of the most stable polymorph.

To summarize, the polymorphic behavior of POP/OOP mixtures resulted in the following:

1. Two polymorphs, α and β', were observed in pure OOP, and the long spacings were 5.7 and 6.4 nm.

The most stable form of OOP was the β' form in a triple-chain-length structure.

2. A time-resolved SR-XRD study revealed polymorphic occurrence of the binary mixture in the metastable states. The POP fraction transformed from α to β' with no passage through γ in the presence of OOP.
3. In contrast to the POP/PPO and POP/OPO mixtures in which molecular compounds were formed [7, 10], the POP/OOP mixtures were immiscible in both the metastable and the most stable polymorphic systems, as indicated in Figs. 1 and 3.

The fact that the POP/OOP mixture was immiscible, not forming a molecular compound like the POP/OPO and POP/PPO mixtures, can be explained by taking into account the molecular interactions between POP and OOP in the mixture phases.

In general, the molecular interactions that most influence stabilization of the crystal structures of TAGs containing saturated and unsaturated fatty acid chains are aliphatic chain packing, glycerol conformation, and methyl end stacking [1]. The aliphatic chain packing is formed by the molecular interactions between saturated and unsaturated fatty acid chains, determining the subcell structures, olefinic conformations, and chain-length structures. The glycerol conformation among the glycerol groups determines the overall configuration of the TAG molecules; methyl end stacking may play an important role in organizing the chain inclination and chain-length structure. The formation of a double-chain-length structure in the molecular compounds of POP/OPO and POP/PPO may be due to combined effects of the aforementioned interactions, and the inability to form a molecular compound in the POP/OOP mixture can be explained by the same consideration. Therefore, we started from the glycerol conformations observed in the stable polymorphs of representative TAG crystals.

Figure 7a illustrates the different types of glycerol conformations of two asymmetric units of TAG molecules present in a unit cell of the most stable forms of the TAGs, whose atomic-level crystal structures were determined by X-ray methods. We symbolized the glycerol conformation using the direction of the glycerol group indicated by an arrow, which is defined as the direction between the middle point of two glycerol carbons at the first and third positions and a glycerol carbon at the second position. The directions of the glycerol groups of neighboring molecules in the β form of tricaproylglycerol lie parallel to the chain axis with the opposite turn [15, 16]. The same arrangements were observed in the asymmetric units of the β'_2 form of 1,2-dipalmitoyl-3-myristoyl-*sn*-glycerol, although there were two combinations in the directions of the glycerol groups with an opposite turn and a parallel turn [17]. The directions of the glycerol groups of two TAGs in the β' form of 1,3-dicaproyl-*sn*-2-lauroylglycerol are parallel with an opposite turn, both making a right angle with respect to the chain axis [18]. The same arrangements were observed in the β form of 1,2-dipalmitoyl-3-acetyl-*sn*-glycerol [19]. The most important property that was commonly observed in the four TAG crystals was the lack of arrangement of unparallel directions of adjacent glycerol groups at right angles to each other. This indicates that such an arrangement must cause instability of glycerol conformations.

Figure 7b illustrates possible glycerol conformations in the molecular compound crystals of mixtures of POP/OPO, POP/PPO, and POP/OOP with double-chain-length structures. The neighboring glycerol groups in a parallel arrangement are directed along the chain axis with an opposite turn in the POP/OPO mixture. This glycerol conformation enables the oleoyl and palmitoyl chains to make separate leaflets with stabilized aliphatic interactions, which may be destabilized when the oleoyl and palmitoyl chains are placed in the same leaflet owing to steric hindrance. The structure may be revealed in molecular compound crystals in the metastable and stable states of POP/OPO [7]. It is inevitable in POP/PPO mixtures that the palmitoyl and oleoyl chains will be located in one leaflet in addition to being present in another leaflet composed of all the palmitoyl chains in the double-chain-length structure. Two situations may occur. In case 1, the adjacent glycerol groups would be directed along the chain axis with an opposite turn, similar to those in the POP/OPO mixture. In case 2, the directions of adjacent glycerol groups would be at right angles to each other. Destabilization in the aliphatic chain packing may be caused in both cases by coexistence of the oleoyl and palmitoyl chains in the two leaflets. However, destabilization may be more enhanced in the structures in case 2, in which the glycerol conformation may be destabilized owing to the unparallel directions of the glycerol groups. Furthermore, the methyl end stacking may also be destabilized owing to unequal chain lengths of the neighboring molecules of POP and PPO, which would again be caused by the unparallel directions of the glycerol groups. Therefore, the molecular compound structure of the POP/PPO mixture observed in the metastable and most stable states [10] may be that of the structural model described in case 1.

We have considered two examples of POP and OOP mixtures. The model of case 1 assumes a parallel direction for the glycerol groups, which may be more stabilized than the unparallel direction in case 2. However, the structural model of case 1 causes destabilization of the acyl chain packing because of the coexistence of oleoyl and palmitoyl chains in the two leaflets. This situation differs significantly from the structural model of case 1 of the POP/PPO mixture, in which the coexistence of oleoyl and palmitoyl chains is limited in either leaflet. An alternative model for POP/OOP is described for case 2, in which the oeloyl and palmitoyl chains are separately placed in their own leaflets. This structure was postulated by Moran [3]. However, this model must cause additional destabilization of the glycerol conformation and unequal chain lengths of the neighboring molecules of POP and OOP, as discussed for case 2 of the POP/PPO mixture. Consequently, neither of the two possible models of the molecular compound structure for a POP/OOP mixture may alleviate destabilization of the acyl chain packing, glycerol conformation, and methyl end stacking. Therefore, no molecular compound has been observed in either the metastable or the stable states in the POP/OOP mixture, as concluded in the present study.

It would be very interesting to examine the effect of the racemicity of OOP, *sn*-1,2-dioleoyl-3-palimitoylglycerol, or *sn*-1-palmitoyl-2,3-dioleoylglycerol on the phase behavior of POP and OOP mixtures. When the mixing behavior differs between two stereoisomers of OOP, further consideration, taking into account the stereospecificity, must be given based on the structural information presented in this paper.

References

1. Larsson K, Quinn P, Sato K, Tiberg F (2006) Lipids: structure, physical properties and functionality. The Oily Press, Bridgewater, pp 9–71
2. Lopez C, Lesieur P, Keller G, Ollivon M (2000) Thermal and structural behavior of milk fat. J Colloid Interface Sci 229:62–71
3. Moran DPJ (1963) Phase behavior of some palmito-oleo triglyceride systems. J Appl Chem 13:91–100
4. Timms RE (1984) Phase behavior of fats and their mixtures. Prog Lipid Res 23:1–38
5. Sato K, Ueno S (2005) In: Shahidi F (ed) Bailley's, industrial oil and fat products, vol 1. Wiley, New York, pp 77–120
6. Koyano T, Hachiya I, Sato K (1991) Phase behavior of mixed systems of SOS and OSO. J Phys Chem 96:716–718
7. Minato A, Ueno S, Yano J, Smith K, Seto H, Amemiya Y, Sato K (1997) Thermodynamic and structural properties of *sn*-1, 3-dipalmitoyl-2-oleoylglycerol and *sn*-1,3-dioleoyl-2-palmitoylglycerol binary mixtures examined with synchrotron radiation X-ray diffraction. J Am Oil Chem Soc 74:1213–1220
8. Engstrom L (1992) Triglycerides systems forming molecular compounds. J Fat Sci Technol 94:173–181
9. Takeuchi M, Ueno S, Sato K (2002) Crystallization kinetics of polymorphic forms of a molecular compound constructed by SOS (1,3-distearoyl-2-oleoyl-*sn*-glycerol) and SSO (1,2-distearoyl-3-oleoyl-*rac*-glycerol). Food Res Int 35:919–926
10. Minato A, Ueno S, Smith K, Amemiya Y, Sato K (1997) Thermodynamic and kinetic study on phase behavior of binary mixtures of POP and PPO forming molecular compound systems. J Phys Chem B 101:3498–3505
11. Timms RE (2003) Confectionery fats handbook, properties, production and application. The Oily Press, Bridgewater, pp 110–119
12. Mihara H, Ishiguro T, Fukano H, Taniuchi S, Ogino K (2004) Effect of crystallization temperature of palm oil on its crystallization. J Oleo Sci 53:231–238
13. Miura S, Konishi H (2001) Crystallization behavior of 1,3-dipalmitoyl-2-oleoyl-glycerol and 1-palmitoyl-2, 3-dioleoyl-glycerol. Eur J Lipid Sci Technol 103:804–809
14. Sato K, Arishima T, Wang ZH, Ojima K, Sagi N, Mori H (1989) Polymorphism of POP and SOS. I. Occurrence and polymorphic transformation. J Am Oil Chem Soc 66:664–674
15. Jensen LH, Mabis AJ (1963) Crystal structure of β-tricaprin. Nature 197:681–682
16. Jensen LH, Mabis AJ (1966) Refinement of the structure of β-tricaprin. Acta Crystallogr 22:770–781
17. Sato K, Goto M, Yano J, Honda K, Kodali DR, Small DM (2001) Atomic resolution structure analysis of β' polymorph crystal of a triacylglycerol: 1,2-dipalmitoyl-3-myristoyl-*sn*-glycerol. J Lipid Res 42:338–345
18. van Langevelde A, van Malssen K, Dressen R, Goubits K, Hollander F, Peschar R, Zwart P, Schenk H (2000) Structure of $C_nC_{n+2}C_n$-type (n = even) β'-triacylglycerols. Acta Crystallogr Sect B 56:1103–1111
19. Goto M, Kodali DR, Small DM, Honda K, Kozawa K, Uchida T (1992) Single crystal structure of a mixed-chain triacylglycarol: 1,2-dipalmitoyl-3-acetyl-*sn*-glycerol. Proc Natl Acad Sci USA 89:8083–8086